## SPPLEMENTAL MATERIAL

### 1. Methods:

*Animal model, drugs, and diets*. Male LDLR null ($LDLR^{-/-}$) mice on a C57BL/6 background and wild-type C57/BL/6 mice were purchased from Jackson Laboratory (Bar Harbor, Maine). At 14 weeks of age, the $LDLR^{-/-}$ mice (n=48) were randomly assigned to one of three treatment groups (vehicle, ritonavir, or ritonavir plus acipimox). The protocol of animal use for this study has been approved by the IACUC of Boston University School of Medicine.

Ritonavir was administered by gavages twice daily at a dose of 33 mg/kg/day, similar to the dose used in published mouse studies [1]. In preliminary experiments, the plasma ritonavir concentration, measured by a modified HPLC method [2], ranged from 3.46 – 7.93 μM (SD 0.86, n=8) in 2 h after drug ingestion, and from 0.23 – 1.83 μM (SD = 1.91, n = 6) in 5 h after drug ingestion. These values are well within the therapeutic range in humans taking ritonavir [3-4]. Acipimox was supplied in drinking water (0.05% wt/wt) and changed twice a week. The average water consumption was about 4 ml per day, equivalent to 2 mg/day intake of acipimox. This dose has been shown to inhibit adipocyte lipolysis in rodents [5-6]. In humans, acipimox is well tolerated beyond 2250 mg/day [7].

Ritonavir has been shown to induce aortic lesions in $LDLR^{-/-}$ mice given a standard mouse chow [8]. However, the lesions thus formed are microscopic and unlikely to cause clinical events. In contrast, an *ad libitum* atherogenic diet induces massive aortic lesions in $LDLR^{-/-}$, as well as other mouse models of atherogenesis, and hence may mask the pro-atherogenic effects of the antiviral drugs (preliminary studies, data not shown). To overcome this problem, we used a modified dietary regimen in which a high fat, high cholesterol (HFC) diet (Harlan Teklad TD.94509) was fed on either two (28% of the time, n = 8) or three (43% of the time, n = 8) days each week interspersed with standard chow (PurinaOne 5051) on the remaining days. Additional pilot tests showed that the pro-atherogenic effect of ritonavir was properly detected under these dietary conditions (data not shown). The HFC diet contains 36.9% kcal from fat, 20.4% kcal from protein, and 41.2% kcal from carbohydrate, with 1.25% wt/wt cholesterol. These diet regimens better mimic the usual dietary fluctuations in free-living animals and humans and allow efficient detection of atherogenic effects of ritonavir (see below).

*Body composition measurement and fat cell size determination.* Longitudinal changes in fat mass were measured in mice using EchoMRI-700/100 whole body composition analyzer (Echo Medical Systems, Houston, Texas). After euthanasia, fat pads were dissected from the subcutaneous, epididymal and perirenal depots. Fat pad weight was expressed as % total body mass. A small section of each fat pad was fixed in buffered 10% formalin and cut into 10 μm sections after parafilm embedding. Fat cell distribution was imaged and analyzed using Metamorph software.

*Magnetic resonance angiography (MRA)*. Mice anesthetized with Isoflurane (0.5%~2% in oxygen) were immobilized inside an MR probe designed for mouse imaging on an 11.7 T Avance spectrometer (Bruker, Billerica, MA). MRA was performed using the 3D FLASH (Fast Low Angle SHot) angiographic sequences. Innominate and right subclavian branch arteries were selected as the comparison sites because mouse atherogenesis typically begins near this branch as a result of the relatively fast and more turbulent blood flow in these areas [9-11].

*Aortic lesion detection.* The aorta was dissected from the arch to the ileal bifurcation, the extraneous tissue was removed, and the intimal surfaces were exposed longitudinally. The aorta was incubated for 5 minutes with Sudan IV (0.5% wt in acetone) and washed three times with 75% ethanol. Sudan IV imparts a red color to the lipid-rich lesions. The aortas were digitized with a CCD camera and lesions on the intimal aortic surface were quantified using Image J software. Representative results of en face staining are shown in Figure II-III. The calculated lesion score shown in Figure 1B are means of N = 8 for each group that were fed HFC 2 days per week. Except for Figure IIIB, all other results shown in this work are from animals given a HFC for 2 days per week.

*Histology and Immunohistochemistry.* Separate experimental mice were prepared for this experiment with 2 d/wk HFC with daily ritonavir dosing and acipimox the same as described above. Experiment was ended after 12 week of treatment. Immediately after mice were euthanized, a catheter was inserted into the left ventricle of the heart and vascular system was flushed 20 ml with PBS followed with 20 ml PBS-buffered 10% formalin. The perfusion was controlled through syringe pump at rate of was 5 ml/min. The heart and the whole aorta was then taken out and dissected clean. The aorta was cut off midway between the root and the Innominate artery. The aorta root was dissected out as ~ 2 mm ring near the valve and embed in paraffin after dehydration. Serial 5 μm sections covering the 300 μm of the proximal aorta, starting from the sinus, were collected. Tissue sections were rehydrated and subjected to antigen retrieval by incubation with 0.1 M sodium citrate (pH 4.5 – 6.2) at 120$^{o}$C using a pressure cooker. After antigen retrieval, tissue slices were process using Zymed HistoMouse-SP Kit (AEC, Broad Spectrum, Invitrogen Cat#959544), following the manufacturer's instructions. Antibody for Mac3 was purchased from BD Biosciences (#550292; San Jose, CA). The first antibody was diluted in 1% BSA at experimentally optimized mixing ratio (1:20 dilute) and incubated with lesion sections at 4$^{o}$C over-night. Positive controls were performed using mouse lymph nodes. Negative controls were performed the same but with mouse IgG. The tissue sections were mounted and photographed using Olympus camera (magnification specified by an in-photo mark, Figure IV). Results were estimated by multiple individuals blinded to the test conditions. Each data point shown in Figure 1C is an average of 3 estimates on the same section. Tissue sections from six different animals were analyzed for each group. These mice were given HFD two days per week for 14 weeks.

Liver histology was performed using formalin-fixed tissue samples, paraffin-embedded, followed with standard sectioning and H&E staining.

*Insulin tolerance test*. Mice were tested between 6 – 8 weeks after drug intervention. Acute and chronic drug effects were tested after administration of the last ritonavir dose in 2 h or 16 h, respectively. Insulin tolerance tests were performed as we described before [12] except that insulin dose was slightly reduced (0.6 U/kg). Acute insulin response is measured as sequential decrease in plasma glucose concentrations. Accumulative insulin response is estimated by the area-under-curve (AUC) of the glucose – time relationship, using the GraphPad Prism software. The two insulin tolerance tests were performed 2 weeks apart to allow the mice a full recovery between tests.

*Lipolysis:* Wild-type C57BL/6 mice (male, 2 month old) were treated with ritonavir (50 mg/kg/day) for 4 weeks. Fat cell isolation and lipolysis assay were performed as previously described [13]. Lipolysis was initiated by adding 50,000 fat cells into 0.5 ml KRH-buffer (pH 7.4, glucose 5 mM) containing vehicle (0.1% ethanol), Isoproterenol (0.5

μM), insulin (1.7 nM), ritonavir (10 μM), and acipimox (0.05%), as noted. After incubation at 37°C for 90 min with gentle shaking (60 Hz), 50 μl of solution was removed for measurement of glycerol. Results were expressed as the amount of glycerol released per min per $10^6$ cells.

*Plasma lipid measurement.* Because food intake affects plasma lipid concentrations, blood sampling was performed on Friday, the last day of chow diet in the week. Mice were fasted from 8:00 AM to 3:00 PM, which approximates an overnight fast in humans. Insulin sensitivity was assessed as plasma FFA responses before and 30 min after insulin injection (0.6 U/kg, tail-vein). Preliminary studies indicated a linear insulin effect on plasma FFA from 15 min to 45 min post injection. Blood was withdrawn from retroorbital vein under light isoflurane anesthesia. Plasma FFA was measured using commercial reagents (Wako NEFA Kit). Plasma samples used for FPLC analysis were withdrawn on the 4th day of chow diet either at 10:00 – 11:00 am (non-fasting) or at 3:00 - 4:00 pm (fasting from 8:00 am to 4:00 pm). The FPLC analysis was performed in the Emory Lipid Research Laboratory of Cardiovascular Specialty Labs, Inc (Atlanta, Georgia). Results are presented as mean +/- SE, with N = 8 for each treatment group. All blood work was done in week 8th – 13th of drug treatment.

*Liver and adipose tissue mRNA analysis*. Total RNA isolation for liver was done using RNAeasy Kit and that for fat tissue was done using RNAeasy kit for lipid rich tissue, following manufacturer's instruction. Both kits were from Qiagen Inc. First strand cDNA synthesis and real-time PCR were done as described in our previous work [13].

*Statistics:* Data are presented as means ± SE. Comparison of means between two groups was performed by using Students' t-test. One-way ANOVA was used for comparison of multiple groups. If ANOVA revealed a significant overall effect at the alpha level of 0.05 or less, individual groups were compared by Tukey's HSD test. All statistics were conducted using the SPSS program.

**References**


1. Goetzman ES, Tian L, Nagy TR, Gower BA, Schoeb TR, Elgavish A, Acosta EP, Saag MS, Wood PA. HIV protease inhibitor ritonavir induces lipoatrophy in male mice. AIDS Res Hum Retroviruses. 2003; 19:1141-1150.
2. Yan Q, Hruz PW. Direct comparison of the acute in vivo effects of HIV protease inhibitors on peripheral glucose disposal. J Acquir Immune Defic Syndr. 2005; 40:398-403.
3. Rudich A, Ben-Romano R, Etzion S, Bashan N. Cellular mechanisms of insulin resistance, lipodystrophy and atherosclerosis induced by HIV protease inhibitors. Acta Physiol Scand. 2005; 183:75-88.
4. Hruz PW, Yan Q. Tipranavir without ritonavir does not acutely induce peripheral insulin resistance in a rodent model. J Acquir Immune Defic Syndr. 2006; 43:624-625.
5. Carballo-Jane E, Gerckens LS, Luell S, Parlapiano AS, Wolff M, Colletti SL, Tata JR, Taggart AK, Waters MG, Richman JG, McCann ME, Forrest MJ. Comparison of rat and dog models of vasodilatation and lipolysis for the calculation of a therapeutic index for GPR109A agonists. J Pharmacol Toxicol Methods. 2007; 56:308-316.
6. Fuccella LM, Goldaniga G, Lovisolo P, Maggi E, Musatti L, Mandelli V, Sirtori CR. Inhibition of lipolysis by nicotinic acid and by acipimox. Clin Pharmacol Ther. 1980;28:790-5.

7. Hannah JS, Bodkin NL, Paidi MS, Anh-Le N, Howard BV, Hansen BC. Effects of Acipimox on the metabolism of free fatty acids and very low lipoprotein triglyceride. Acta Diabetol. 1995; 32:279-283.
8. Dressman J, Kincer J, Matveev SV, Guo L, Greenberg RN, Guerin T, Meade D, Li XA, Zhu W, Uittenbogaard A, Wilson ME, Smart EJ. HIV protease inhibitors promote atherosclerotic lesion formation independent of dyslipidemia by increasing CD36-dependent cholesteryl ester accumulation in macrophages. J Clin Invest. 2003; 111:389-397.
9. Hockings PD, Roberts T, Galloway GJ, Reid DG, Harris DA, Vidgeon-Hart M, Groot PH, Suckling KE, Benson GM. Repeated three-dimensional magnetic resonance imaging of atherosclerosis development in innominate arteries of low-density lipoprotein receptor-knockout mice. Circulation. 2002;106:1716-1721.
10. Choudhury RP, Aguinaldo JG, Rong JX, Kulak JL, Kulak AR, Reis ED, Fallon JT,Fuster V, Fisher EA, Fayad ZA. Atherosclerotic lesions in genetically modified mice quantified in vivo by non-invasive high-resolution magnetic resonance microscopy. Atherosclerosis. 2002;162: 315-321.
11. Feintuch A, Ruengsakulrach P, Lin A, Zhang J, Zhou YQ, Bishop J, Davidson L,Courtman D, Foster FS, Steinman DA, Henkelman RM, Ethier CR. Hemodynamics in the mouse aortic arch as assessed by MRI, ultrasound, and numerical modeling. Am J Physiol Heart Circ Physiol. 2007; 292: H884-H892.
12. Tu P, Bhasin S, Hruz PW, Herbst KL, Castellani LW, Hua N, Hamilton JA, Guo W. Genetic disruption of myostatin reduces the development of proatherogenic dyslipidemia and atherogenic lesions in Ldlr null mice. Diabetes. 2009; 58:1739-748.
13. Wang-Fisher YL, Han J, Guo W. Acipimox stimulates leptin production from isolated rat adipocytes. J Endocrinol. 2002;174:267-272.

# 2. Supplemental Data

**A: 3D abdominal thoracic artery tree**

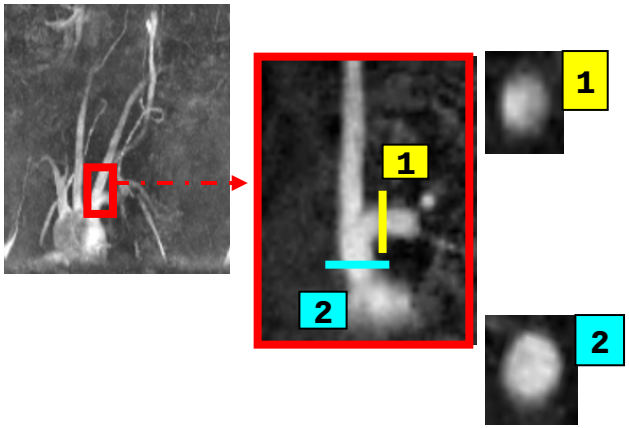


**B: Lipid staining of branch of right subclavin and innominate arteries**

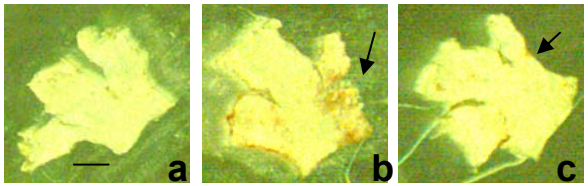


VEH RTV RTV/ACX

**Figure IA: Mouse thoracic aorta with its major branches was viewed by MRA (left). The innominate (2) and right subclavin (1) artery branch (middle) are shown in the middle panel, and the right panel shows the cross-section of innominate (2) and right subclavin arteries near their origin. B: Lipid staining of innominate and right subclavin branch in mice treated for 8 weeks for vehicle (a), ritonvir (b) and ritonvir co-treated with acipimox (c). The arrow marks indicate the lipid-rich lesions stained red after incubation with Sudan IV (bar = 500 mm).**

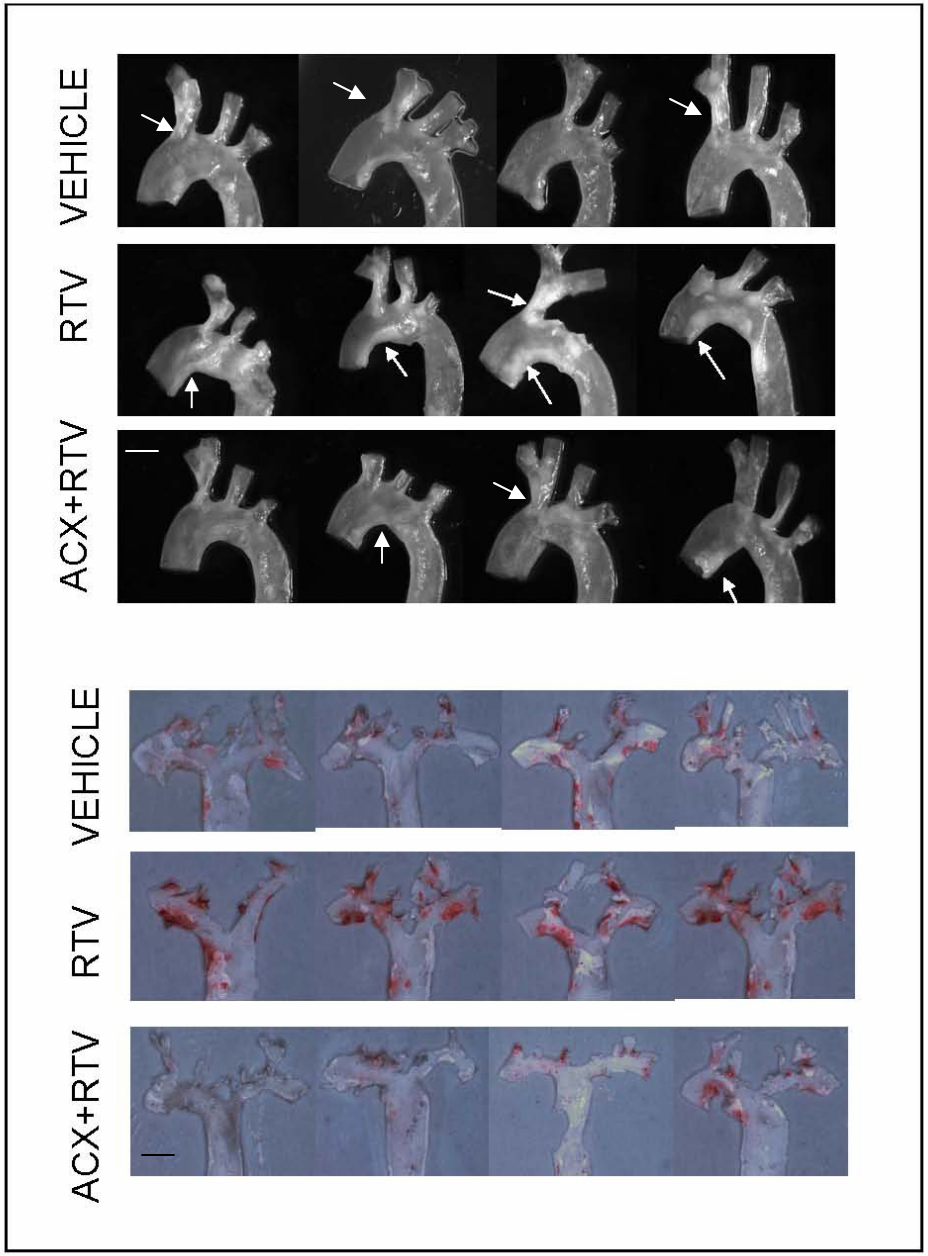


**Figure II. Upper panel: isolated mouse aorta arch with the branches intact. The whitish areas (marked with arrows) reflect athermanous lesions (bar = 1 mm). Lower panel: the en face of aorta arch with lipid lesions stained by Sudan IV (bar = 2 mm). The images are representative of results from N ≥ 8 independent animals. These mice were fed with HFC for 2 days per week. Ritonavir was given twice a day at a dosage of 33 mg/kg/day. Acipimox was given in drinking water at 0.05%. Experiment was completed in 14 weeks.**

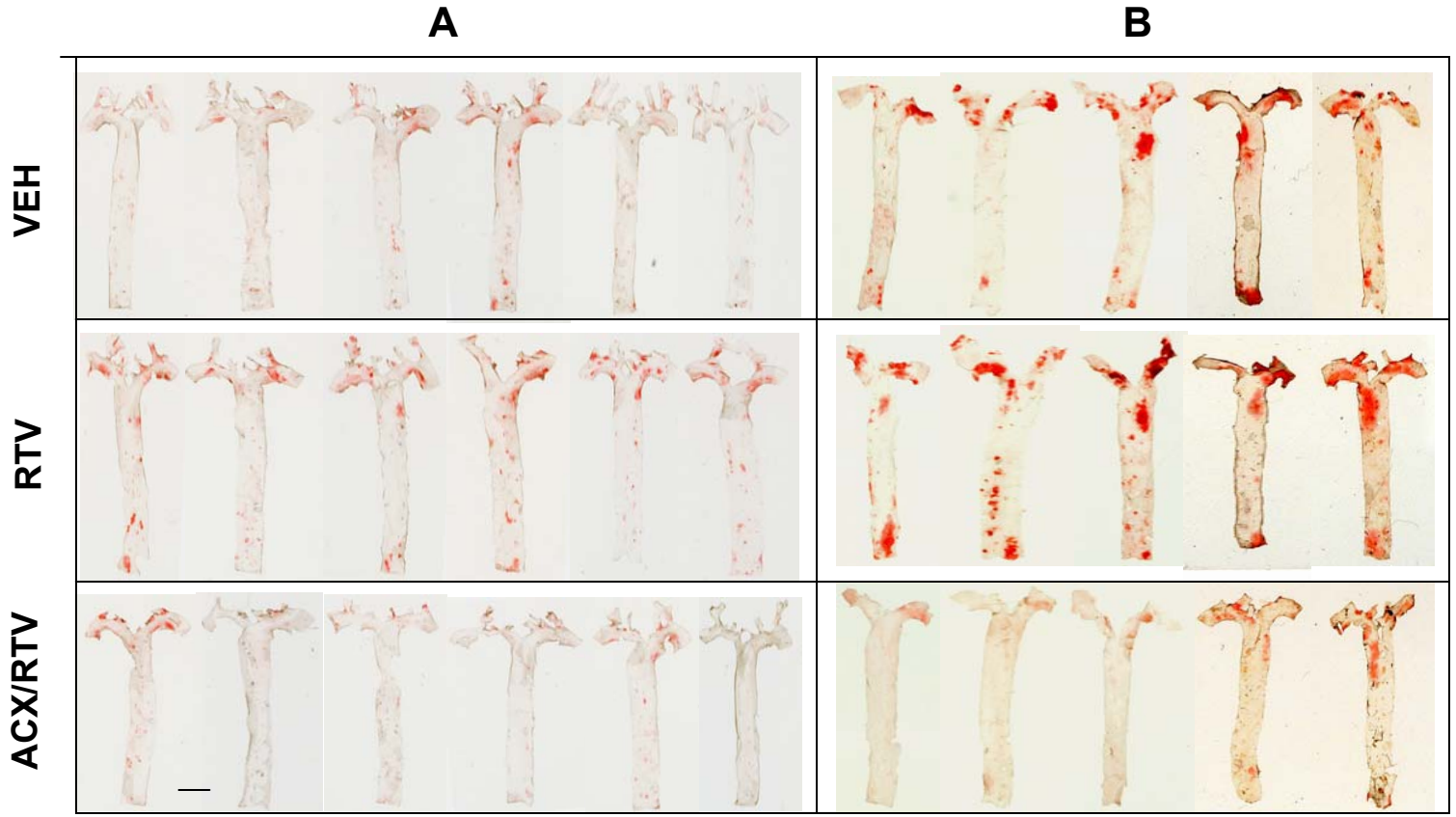


**Figure III: en face detection of lesion distribution throughout the aorta arch and the descending aorta, stained red with Sudan IV (bar = 2 mm). A: isolated aorta from mice treated with HFC for 2 days per week. B: isolated aorta from mice treated with HFC for 3 days per week. All were treated for 14 weeks with drug conditions as described for Figure S2. These results indicate that increased dietary fat intake resulted greater lesion deposits. Since the pro-atherogenic effect of ritonavir and atheroprotective effect of acipimox against ritonavir was clearly demonstrated under both dietary conditions, the following studies were conducted only on animals fed HFC on the 2 days per week schedule.**

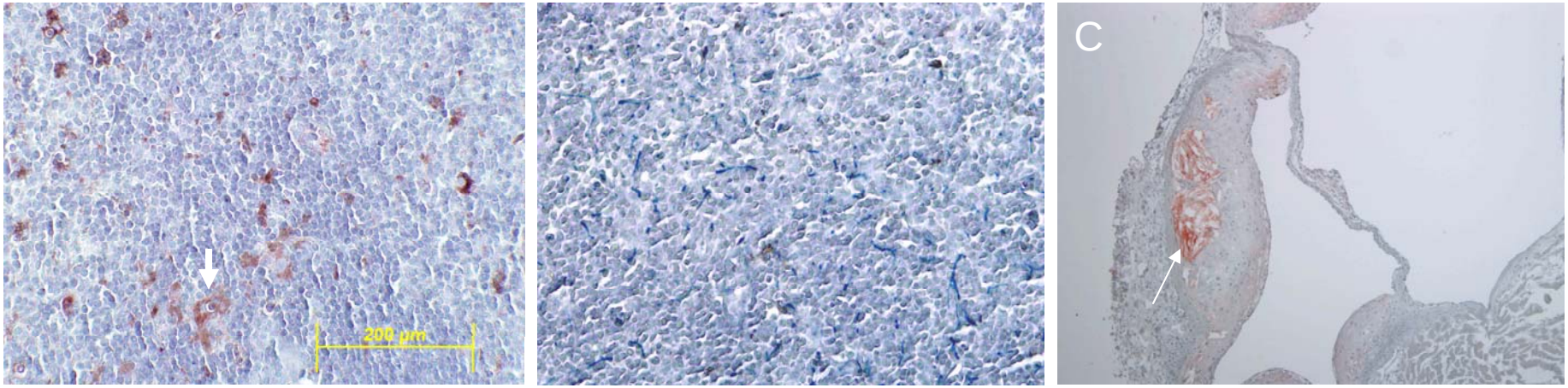


**Figure IV. positive and negative control of IHC staining for Mac3. A&B: lymph node from normal mice was embedded in wax and sectioned into 5 μm. After antigen retrieve, tissue slice was incubated with anti-Mac3 (1:20, A) or mouse IgG (1:20, B) overnight. Subsequent 2nd antibody reaction and substrate color development were performed using Zymed Kit following manufacturer's instruction. The intense dark rusty red spots (arrow) indicates positive staining for Mac3. C: a representative aorta root section after treated with IgG the same as the negative control B. It is noticed that IgG alone stained bright red color in areas of mechanical defects, such as the large necrotic core in (arrow). However, IgG staining is negligible at the foam cell rich areas near the lesion surface, indicating low probability of nonspecific false positive staining in this area.**

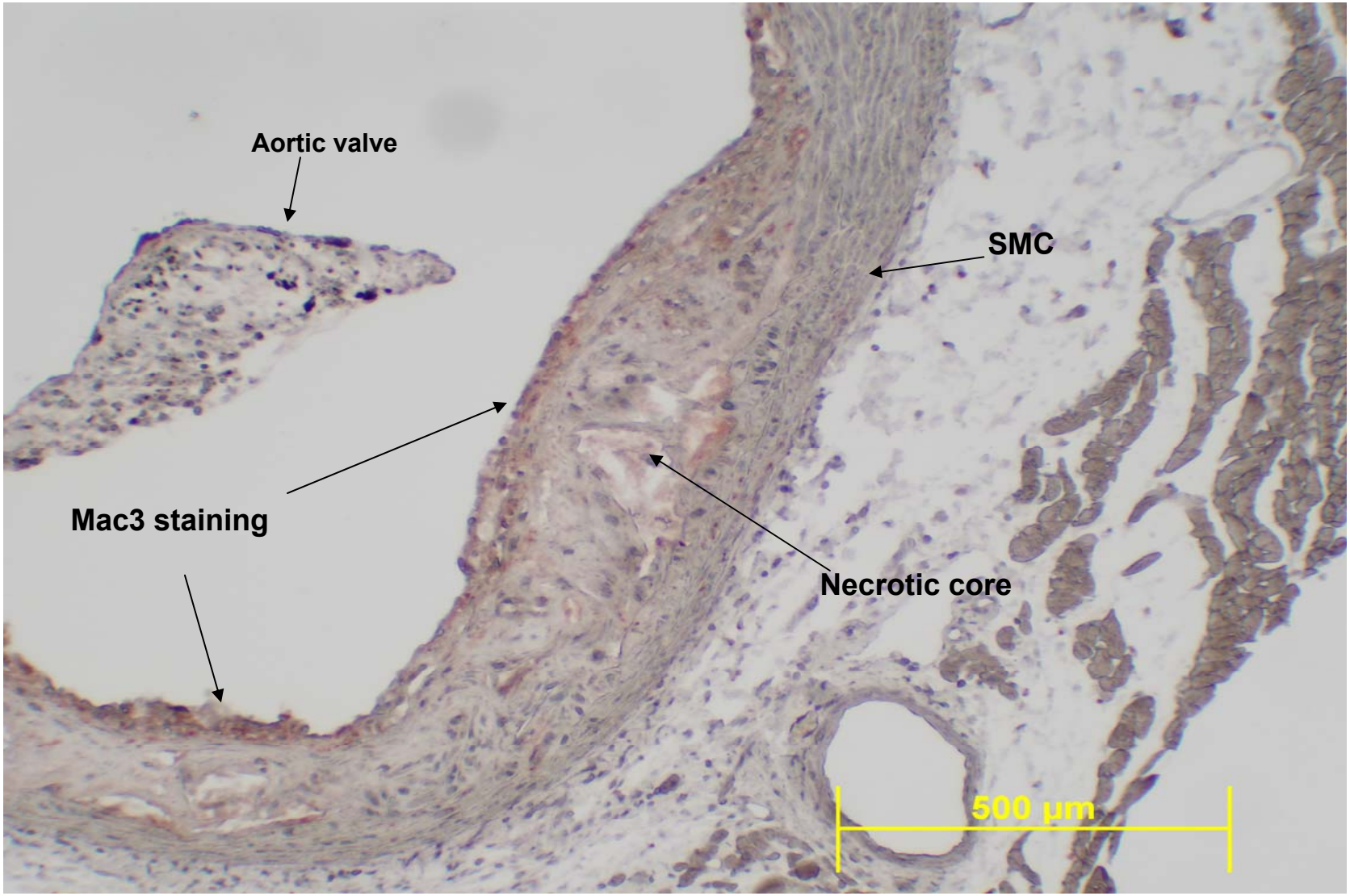


**Figure IV-D (Vehicle group): showing mild to moderate presence of Mac+ macrophages in the area overlaying the lesion core.**

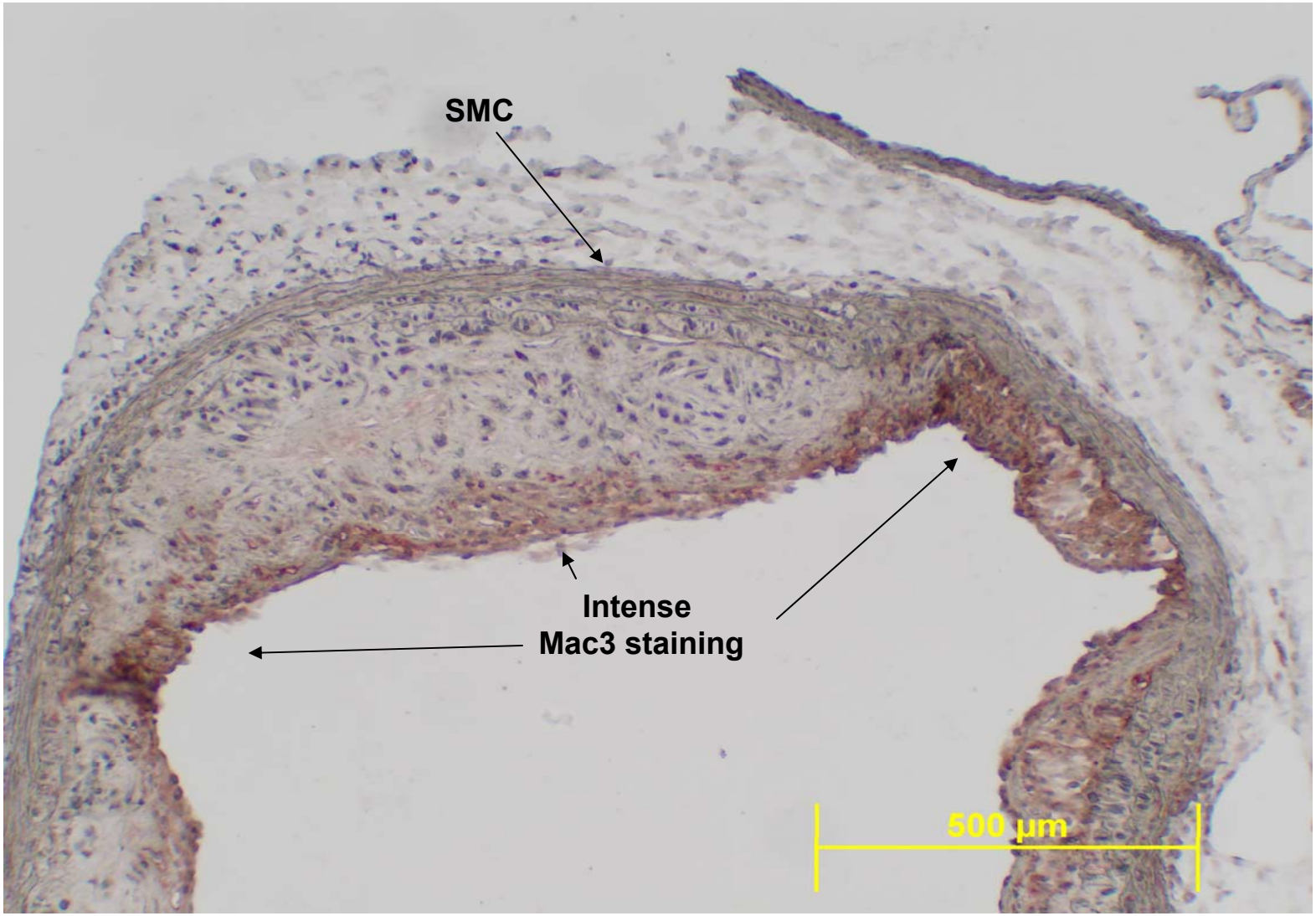


**Figure IV-E (ritonavir group): showing intense presence of Mac+ macrophages in the shoulder area as well as the area overlaying the lesion core.**

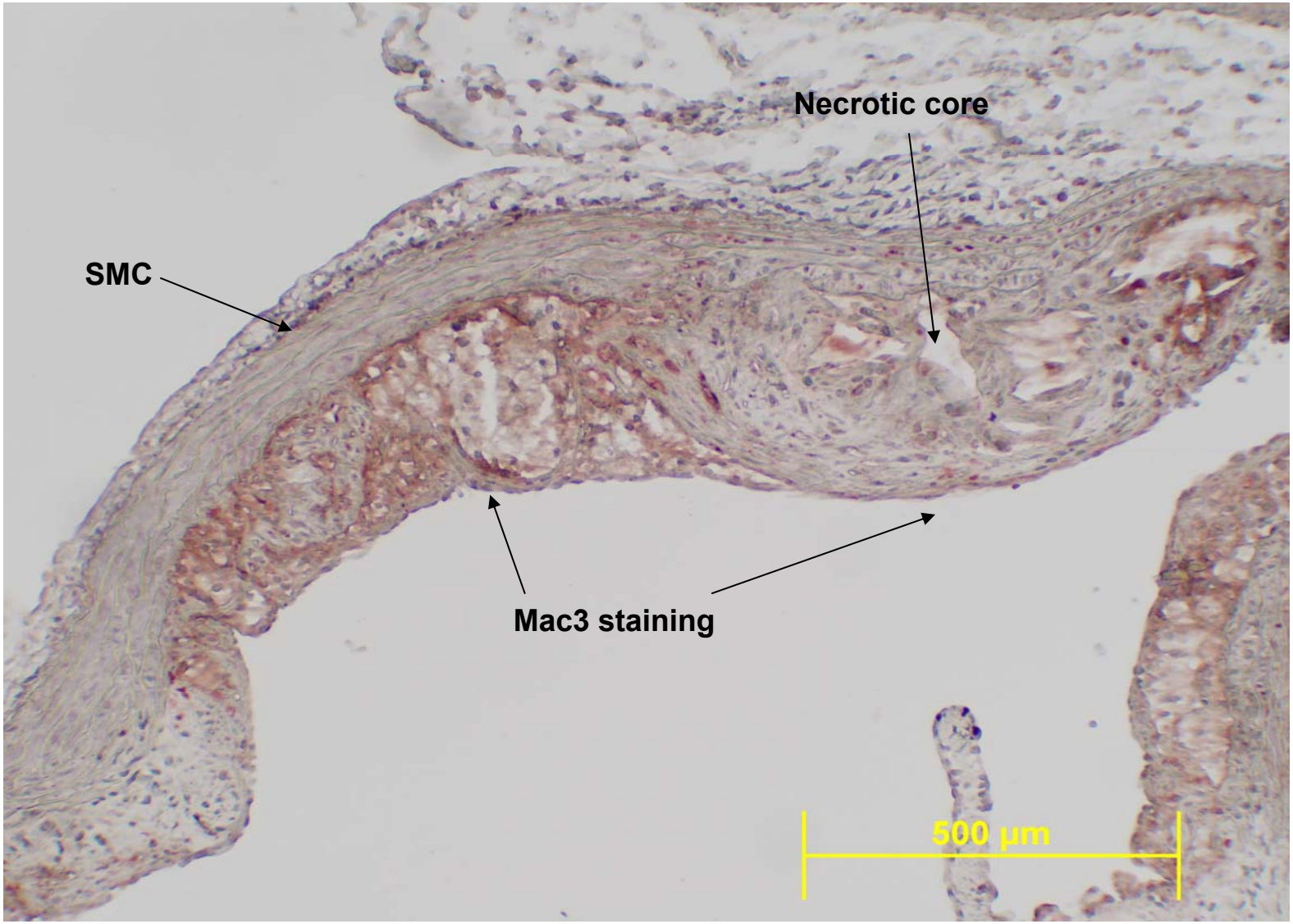


**Figure IV-F (ritonavir plus acipimox group): showing intense Mac3+ staining at the shoulder area but very mild in the area overlaying the lesion core.**

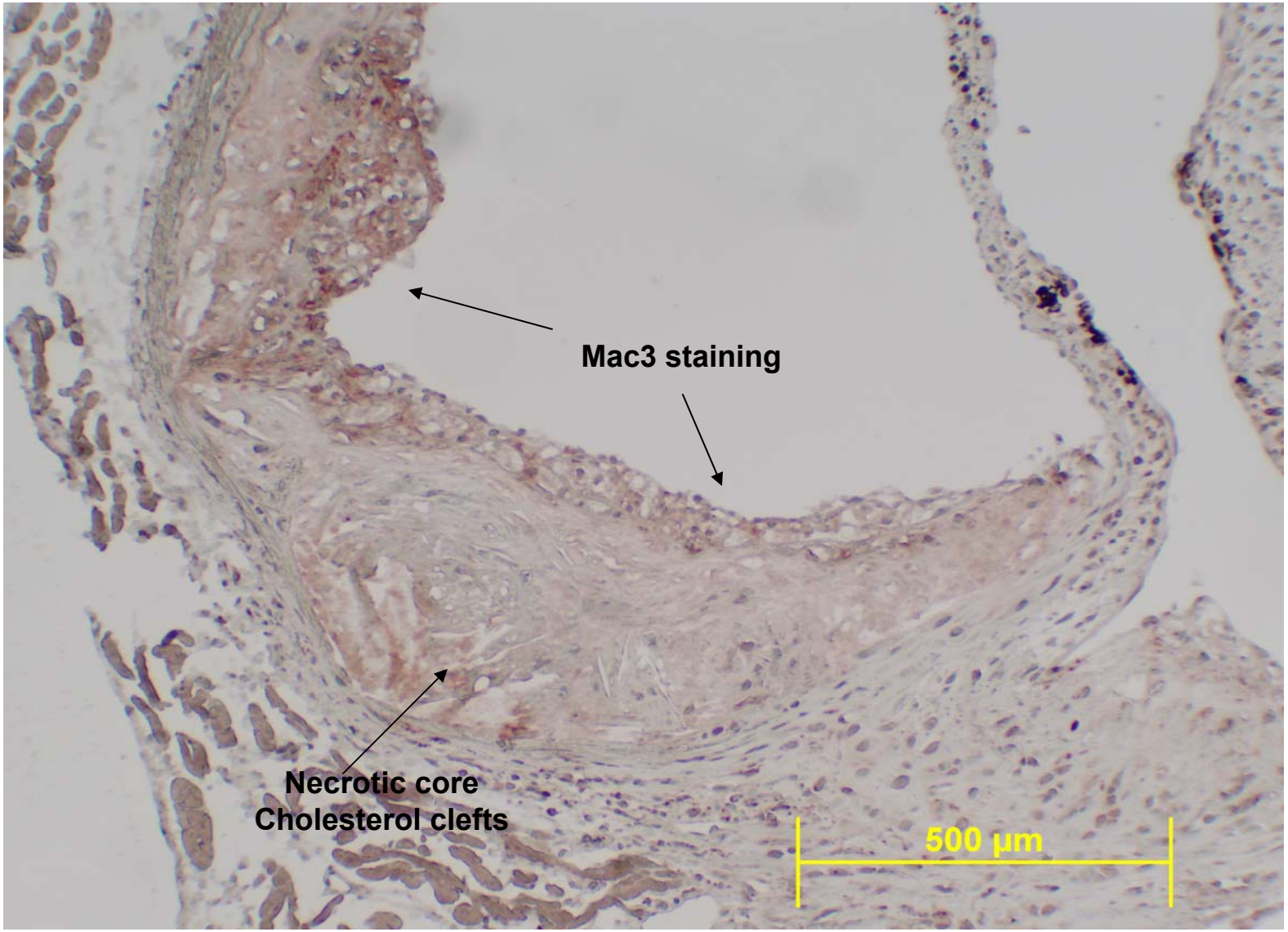


**Figure IV-G (Vehicle group): showing moderate to intense Mac+ staining at the shoulder but mild in the area overlaying the lesion core.**

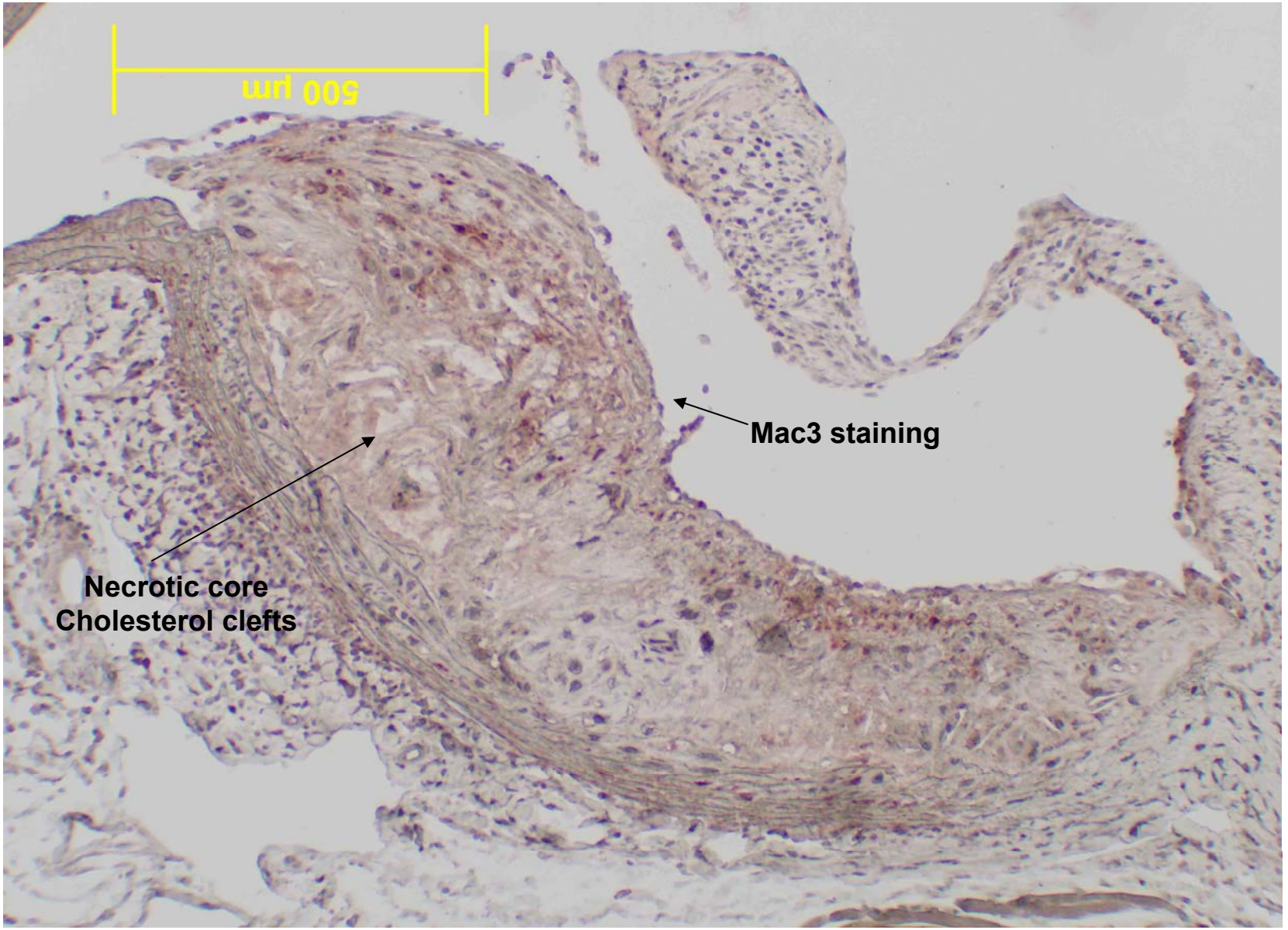


**Figure IV-H (ritonavir group): enlarged lesion core overlaid with think layers of Mac+ staining.**

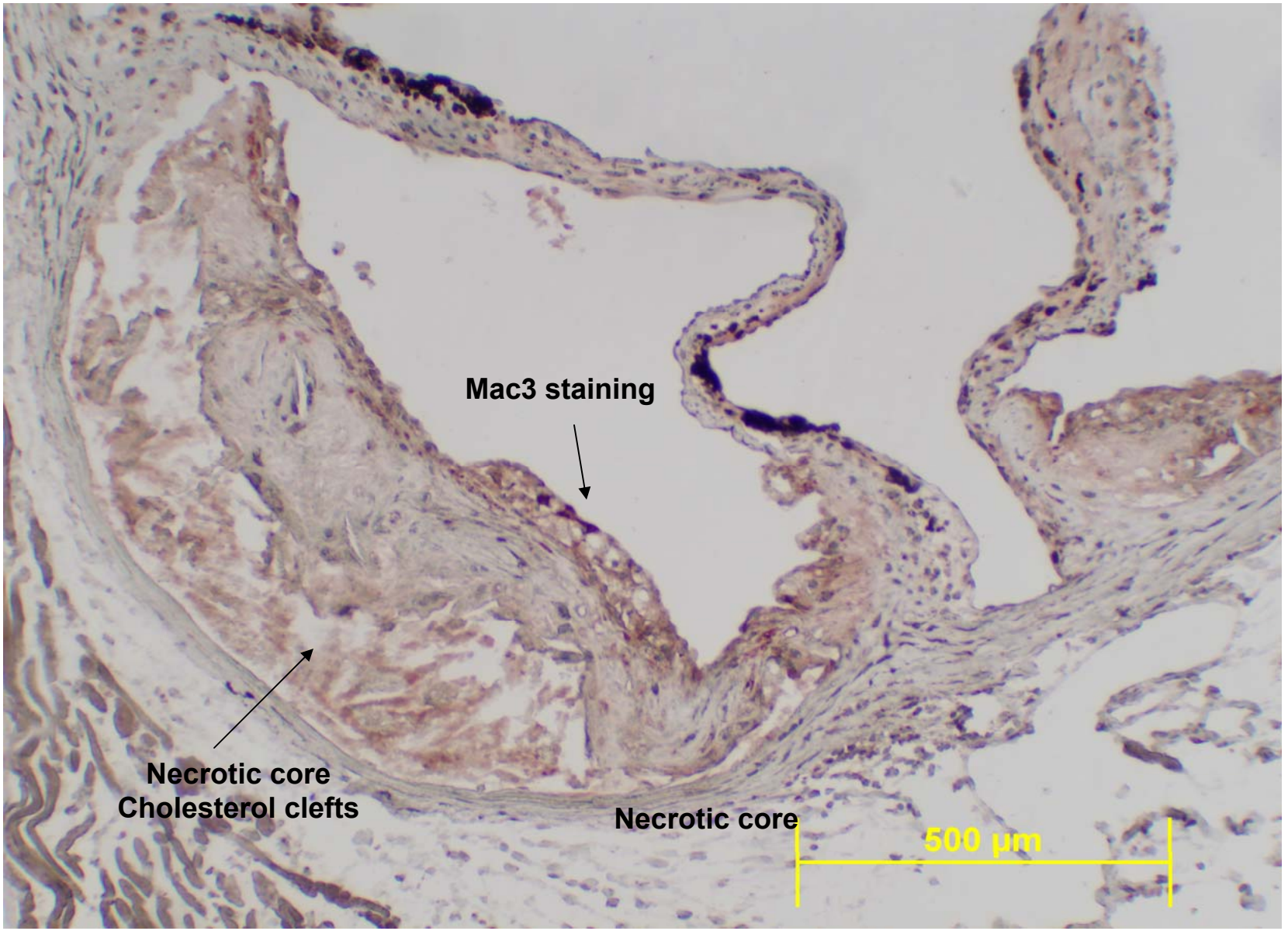


**Figure IV-I (ritonavir plus acipimox group): enlarged lesion with large necrotic core. Moderately intense Mac+ staining near the shoulder. The color within the necrotic core is artificial, possibly due to the rugged texture in the sample area (compared to IgG stained negative control, not shown).**

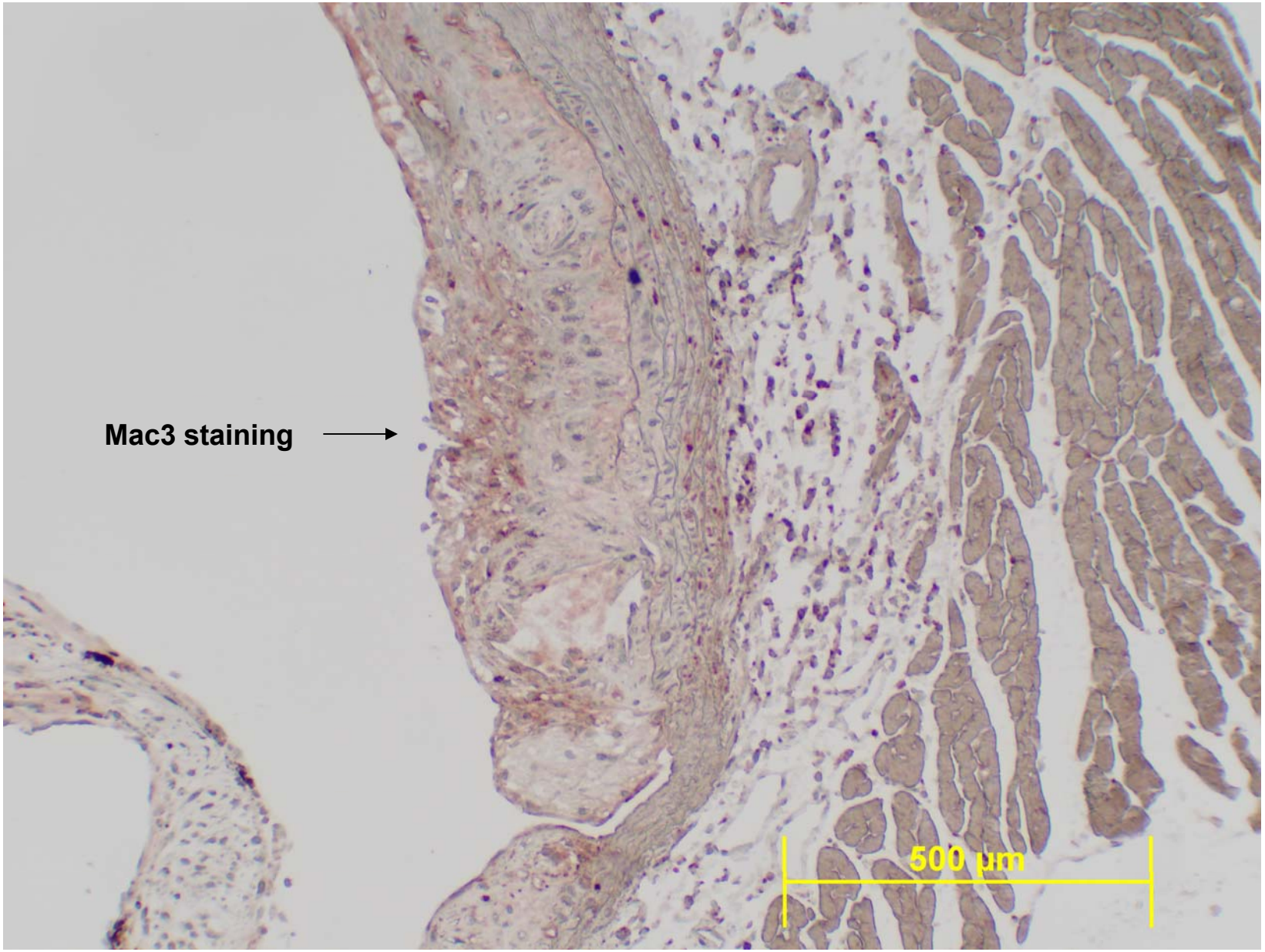


**Figure IV-J (Vehicle group): mild to moderate Mac+ staining overlying the lesion core.**


**Figure IV-K (ritonavir group): intense Mac+ staining in the thickened intima area overlying a moderate size lesion.**

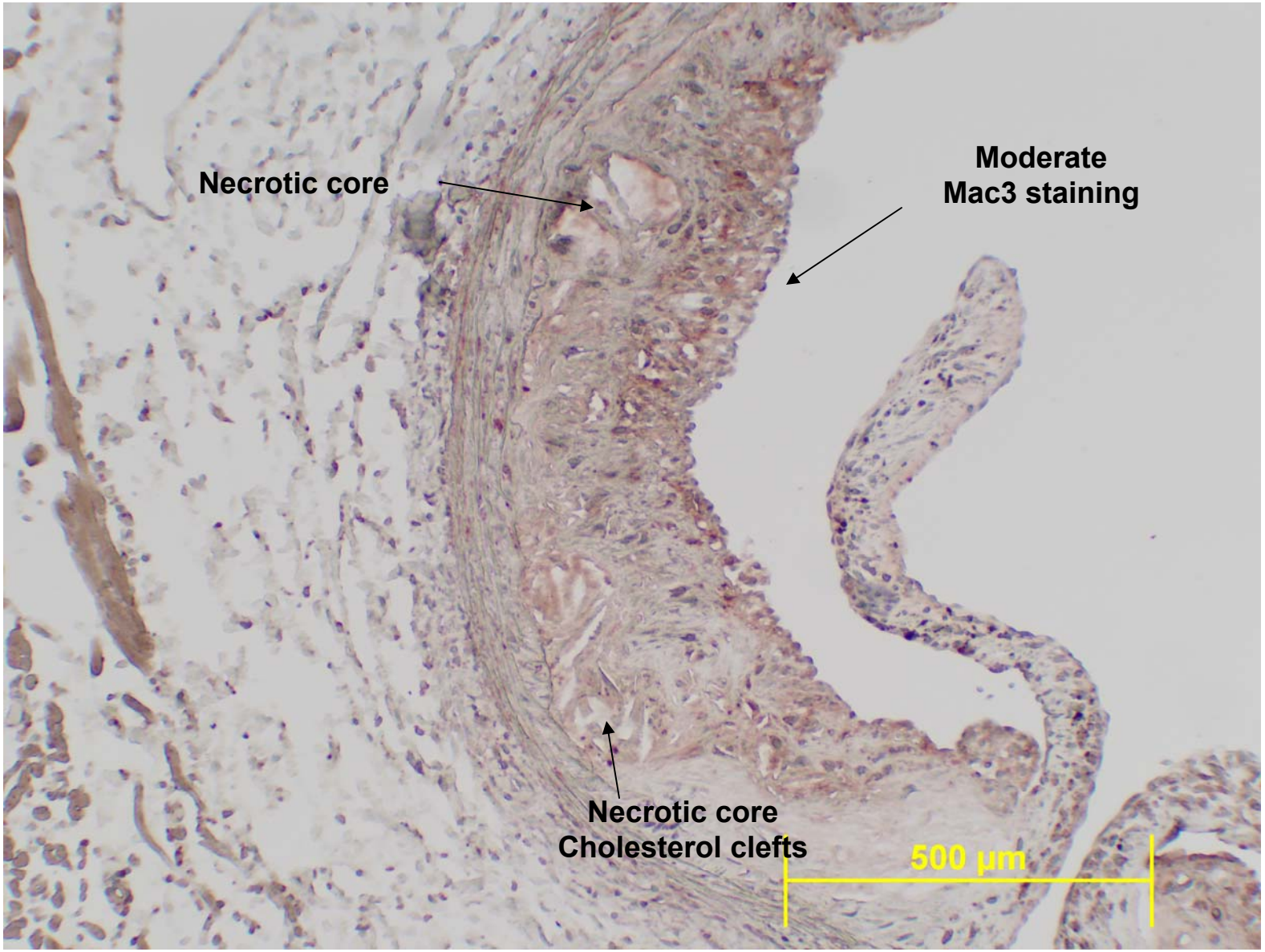


**Figure IV-L (ritonavir plus acipimox group): moderate Mac+ staining in the area overlaying the lesion core.**

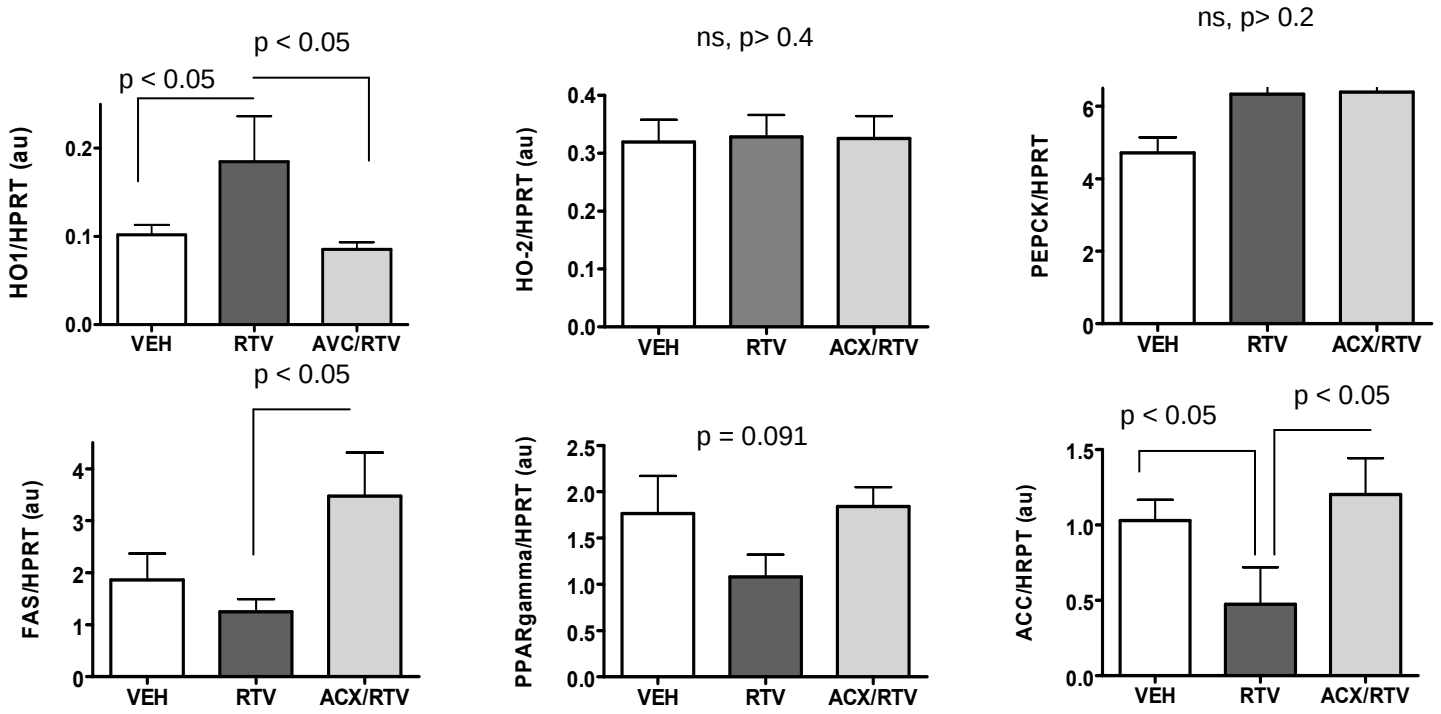


**Figure V: Effects of ritonavir and acipimox on adipose tissue mRNA expression for heme oxygenase-1 (HO-1), HO-2, PEPCK, fatty acid synthase (FAS), PPARgamma, and acetyl CoA carboxylase (ACC). Among which, HO-2 is a constitutive heme oxygenase not subjected to exogenous regulations. It is not surprising that HO-2 is not affected by ritonavir nor acipimox. PEPCK has recently been implicated in lipolysis regulation. However, our results do not suggest an involvement of this enzyme in ritonavir-mediated metabolic effects, at least not at the mRNA level. The observation of suppressed PPARgamma, FAS and ACC by ritonavir suggest that decreased lipogenesis may also contribute to fat mass loss. However, the fact that all these changes were blocked by acipimox suggest that ritonavir modulates fat tissue function through mechanisms that involve lipolysis regulations.**

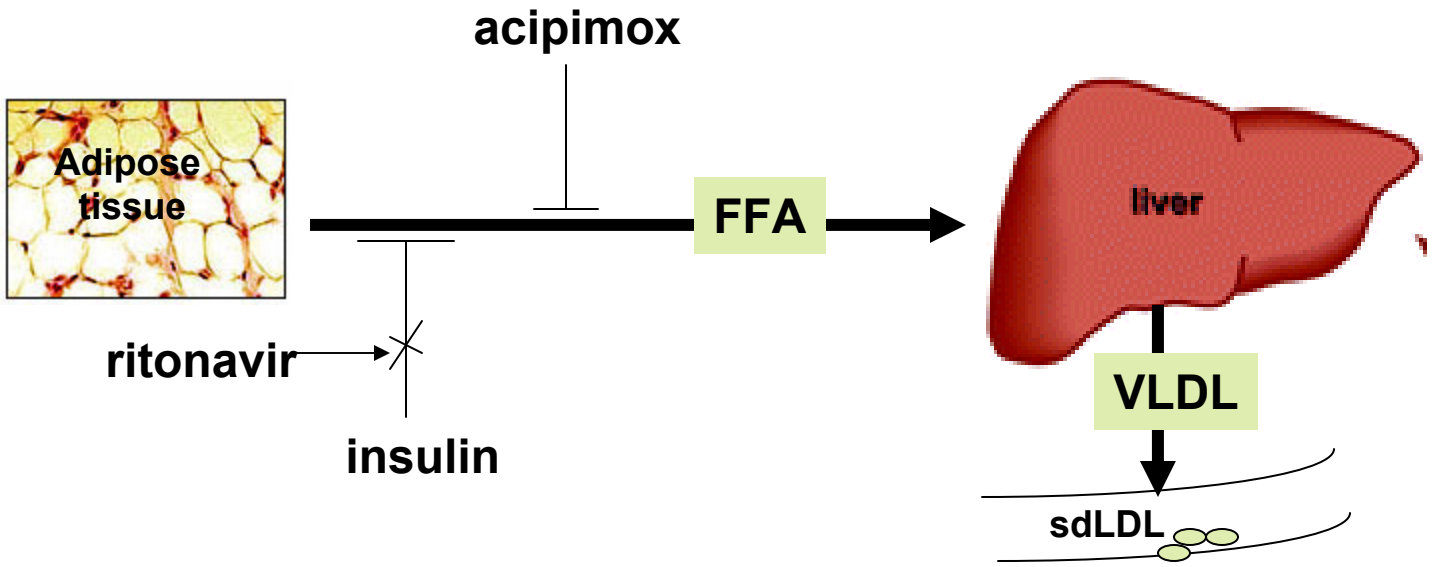


**Figure VI. Illustration of the hypothetical mechanism of ritonavir-mediated proatherogensis and how it is reversed by acipimox.**

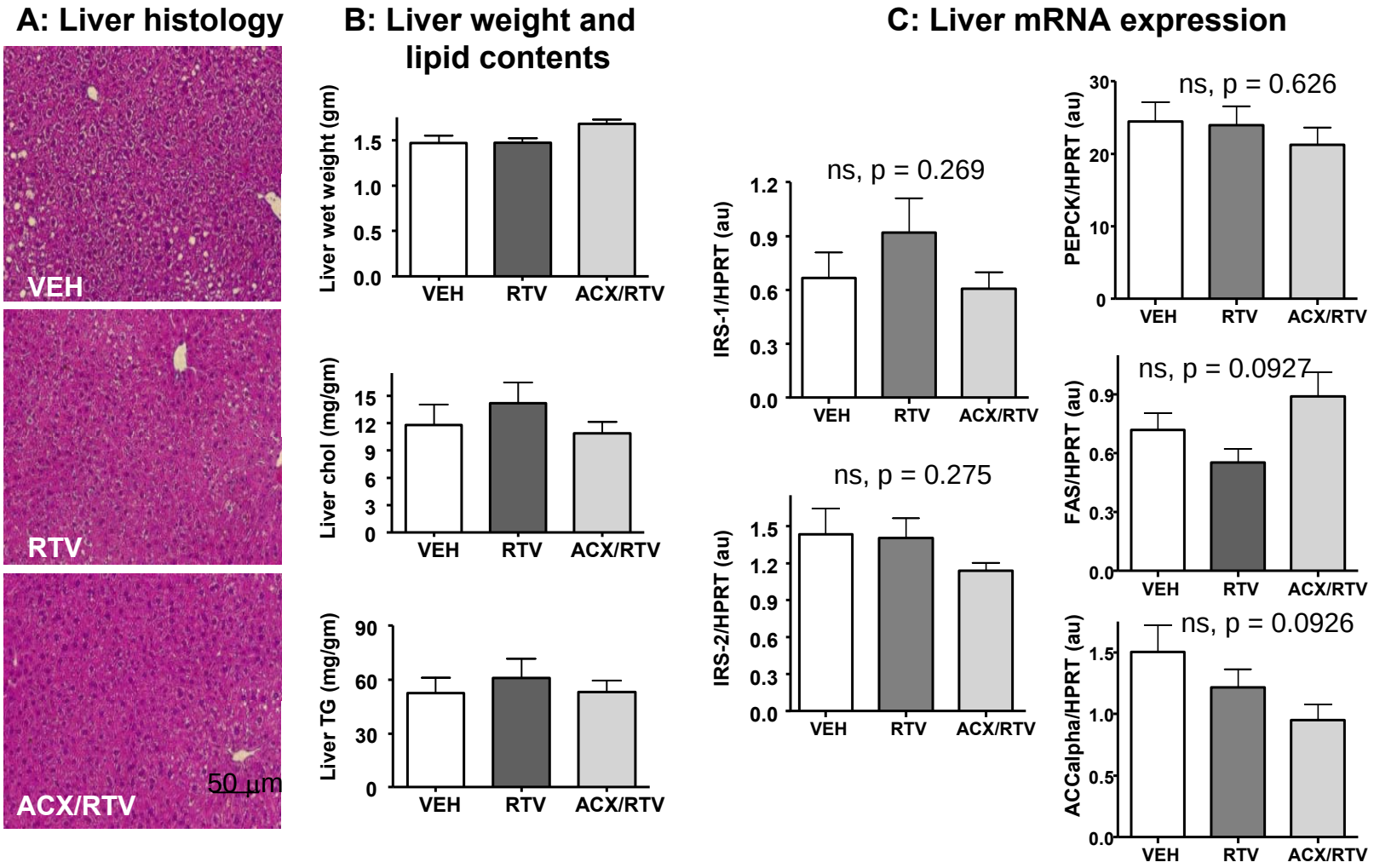


**Figure VII: Liver is not a primary target of ritonavir under the current experimental conditions. H&E staining of liver slice show similar and mild signs of steatosis in all, which was not aggravated by ritonavir or acipimox (A). Neither ritonavir nor acipimox affected liver size and lipid storage (B). Neither ritonavir nor acipimox had significant impacts on insulin receptor substrates IRS1&2 or metabolic genes PEPCK, FAS, and ACC.**